Available online at www.sciencedirect.com

ScienceDirect

Ceramics International 36 (2010) 365–369

CERAMICS INTERNATIONAL

www.elsevier.com/locate/ceramint

Short communication

A comparative study of the properties of terbium aluminum garnet powder sintered in air, vacuum and by laser irradiation

Humyra Shabir [a], Bansi Lal [a,*], M. Rafat [b]

[a] Centre for Laser Technology, Indian Institute of Technology Kanpur, Kanpur 208016, India
[b] Department of Applied Sciences & Humanities, Faculty of Engineering & Technology, Jamia Millia Islamia, New Delhi 110025, India

Received 25 March 2009; received in revised form 27 May 2009; accepted 8 July 2009

Abstract

The structural and optical properties of terbium aluminum garnet (TAG) powder sintered (~1100 °C) in air, vacuum (~10^{-6} mbar) and with 70 W of unfocussed CW CO_2 laser radiation, have been studied using X-ray powder diffraction (XRD), scanning electron microscopy (SEM/TEM), FTIR, optical absorption and photoluminescence techniques. Structural properties of TAG are found to be independent of the sintering procedure except that the pure TAG crystalline phase ($Tb_3Al_5O_{12}$) is evolved in about 2 h in the case of laser sintering compared to 8 h needed in air sintering (by furnace) and 4 h needed in the case of vacuum furnace sintering. On the other hand, the absorption/emission intensity (300–600 nm region) of TAG samples sintered in vacuum is higher compared to that of laser/furnace sintering in air.

Keywords: A. Sintering; D. Terbium aluminum garnet ceramics; Laser irradiation

1. Introduction

Large Verdet constant (180 rad T^{-1} m^{-1}, room temp., 633 nm) and broad transmission range (350–1500 nm) [1] make crystalline terbium aluminum garnet ($Tb_3Al_5O_{12}$; TAG) a material of choice for magneto-optical devices like Faraday rotator, optical isolator, etc. [2]. However, because of its incongruent melting properties, preparation of single crystals suitable for practical applications is still a problem [3]. Alternately, poly-crystalline TAG powder of adequate density and transparency can be used for the realization of optical devices. Saxena et al. [4] reported the synthesis and characterization of submicron sized TAG powder using sol–gel technique while Humyra et al. [5] have been able to synthesize nano-sized poly-crystalline powder by the same technique. In both these studies, the material has been sintered in air using a resistance furnace. In order to realize practically meaningful magneto-optical devices based on poly-crystalline TAG powder, the synthesis process has to be tailored so as to optimize its property(ies) relevant to the application. Sintering is known to play a crucial role in the control and optimization of the properties of the material being synthesized [6]. This study reports the characterization of the TAG powder prepared by a sol–gel technique and sintered (~1100 °C) by (i) resistance furnace in air at atmospheric pressure and at ~1×10^{-6} mbar pressure and (ii) laser in which the sample in the pellet form is irradiated by unfocussed 70 W CW CO_2 laser radiation in air. The nano-sized poly-crystalline TAG thus prepared has been characterized by powder diffraction (XRD), scanning electron microscopy (SEM/TEM), FTIR, optical absorption and photoluminescence techniques.

2. Experimental

2.1. Sample preparation

TAG precursor prepared by a sol–gel technique through the citrate–nitrate route [5], is hand ground in pestle–mortar into fine powder and made into pellets (10 mm diameter and 1.5 mm thick) by a die–hydraulic-press combination.

2.2. Sintering

Sintering in air is carried out in a wire-wound (80% Ni–20% Cr alloy) horizontal furnace while the material is vacuum

---

* Corresponding author. Tel.: +91 512 2597930; fax: +91 512 2597766.
E-mail address: bansi@iitk.ac.in (B. Lal).

0272-8842/$36.00 © 2009 Elsevier Ltd and Techna Group S.r.l. All rights reserved.
doi:10.1016/j.ceramint.2009.07.019

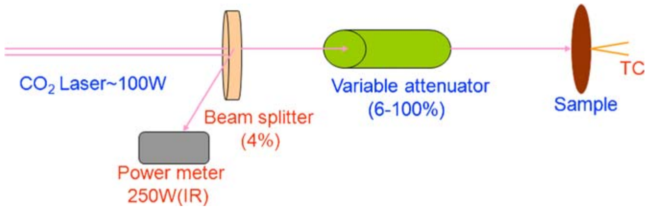

Fig. 1. Schematics of the laser sintering setup.

($\sim10^{-6}$ mbar) sintered in 90% Pt–10% Rh alloy vertical furnace. Both the furnaces are fitted with temperature controllers so as to control the pre-set temperature within ±1 °C.

The experimental arrangement for laser sintering is shown in Fig. 1. In this case the TAG precursor pellet is held in between two graphite plates which have central holes of 6 mm diameter. The laser radiation from a home-built CW CO_2 laser is made to fall without focusing on the pellet through a beam attenuator (variable from 6 to 90%, II–VI Infrared Inc., USA). The beam diameter of the laser is about 6 mm. The nominal power obtainable from the laser is about 90 W with about 2% variation over a period of 6 h.

The beam attenuator is set to 6% position so that ~6 W of CO_2 laser radiation is made to fall on the pellet for about 15 min after which power is increased to 10 W with exposure time of 15 min. This is continued for about 1 h till the sample is finally irradiated with 80 W of CW power for 1 h and subsequently naturally cooled to room temperature. The temperature of the pellet monitored with a type K-thermocouple, is about 1100 °C with 80 W irradiation.

2.3. Characterization

Powder XRD spectra in the range 15–75° have been recorded by JSO-Debye flex 2002 X-ray diffractometer using 1.5418 Å Cu Kα radiation, 3° min^{-1} scanning speed and 0.03 step size.

SEM analysis has been carried out using ZEISS Supra 40 VP FESEM system while FETEM images have been recorded on TECNAI G2, U-twin HRTEM system using 200 kV accelerating voltage. To prepare the sample, powders are dispersed in ethanol using an ultrasonic horn. For SEM analysis a drop of this mixture is allowed to dry on silicon wafer followed by gold coating (for ~10 min) while for FETEM recording, a drop of the mixture is dried on carbon coated copper grid.

FTIR spectra in 400–4000 cm^{-1} region have been recorded with Bruker Optics USA Model Vertex 70 spectrophotometer using the KBr pellet (~1 wt% sample) method.

Room temperature excitation and photoluminescence spectra in the range 300–600 nm have been recorded with Jobin-yvon Model Fluorolog-3 fitted with Xe lamp as the excitation source.

3. Results and discussion

3.1. Structural properties

Powder XRD spectra of the TAG powder sintered at ~1100 °C in air, vacuum ($\sim10^{-6}$ mbar) and by laser radiation are shown in Fig. 2. The XRD patterns have been indexed as $Tb_3Al_5O_{12}$ phase (JCPDS # 17-0735). The average size of the crystallites calculated by the well-known Scherrer equation is found to be 24.61 nm for air-sintered samples, 25.93 nm for vacuum sintered and 24.92 nm for the laser sintered samples implying that the structure of the end-product (TAG) is almost the same with all the three types of sintering. This conclusion is further confirmed by SEM, TEM and FTIR studies. Typical SEM micrographs of the TAG samples sintered in air by furnace/laser and in vacuum are shown in Fig. 3. As seen in this figure, the surface morphology of samples is independent of the sintering technique adopted. However, it needs 8 h sintering time in the case of air sintering by furnace which is reduced to about 4 h when the sample is sintered in vacuum furnace. This sintering time is further reduced to about 2 h in the case of CO_2 laser radiation sintering. This dramatic decrease in sintering time is due to better coupling of laser radiation with the sample where unfocussed laser beam is made to fall directly on the sample.

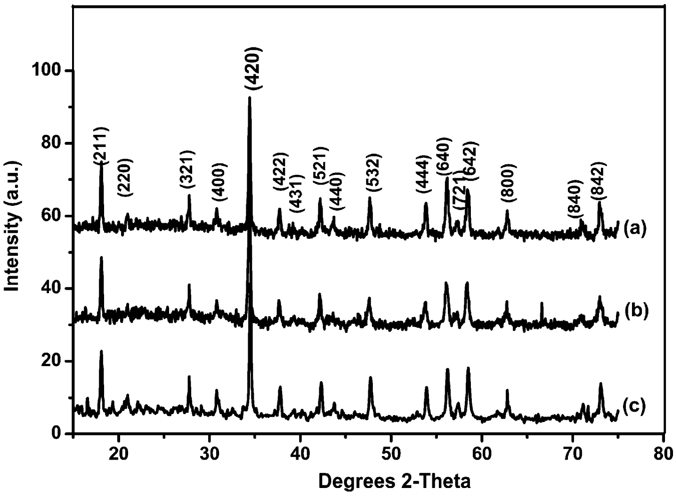

Fig. 2. XRD pattern of TAG powder sintered at 1100 °C (a) in air/furnace for 8 h, (b) in vacuum ($\sim10^{-6}$ mbar) furnace for 4 h and (c) by laser irradiation in air for 2 h.

Fig. 4 shows a typical transmission electron microscope (TEM) image of a TAG sample sintered in air (furnace) at 1100 °C. The selected area electron diffraction (SAED) pattern (inset in Fig 4) of the corresponding sample shows that the particles are poly-crystalline in nature. The size of the samples observed from TEM micrographs is in good agreement with the sizes obtained from the XRD patterns. Similar results have been observed in the case of laser/vacuum sintered samples.

The FTIR spectra recorded in air, of the three representative samples of TAG are shown in Fig. 5. All the three spectra have similar features showing that the molecular structure as well as the chemical bonding of the samples sintered by conventional techniques and by laser irradiation, remains unaffected. The peaks in the lower frequency region at 694, 722 and 788 cm^{-1} are due to metal oxygen bonds (Tb–O and Al–O) vibrations [7,8]. The frequency bands at 1625, 2924 and 3419 cm^{-1} are due to water, etc. present in the atmosphere.

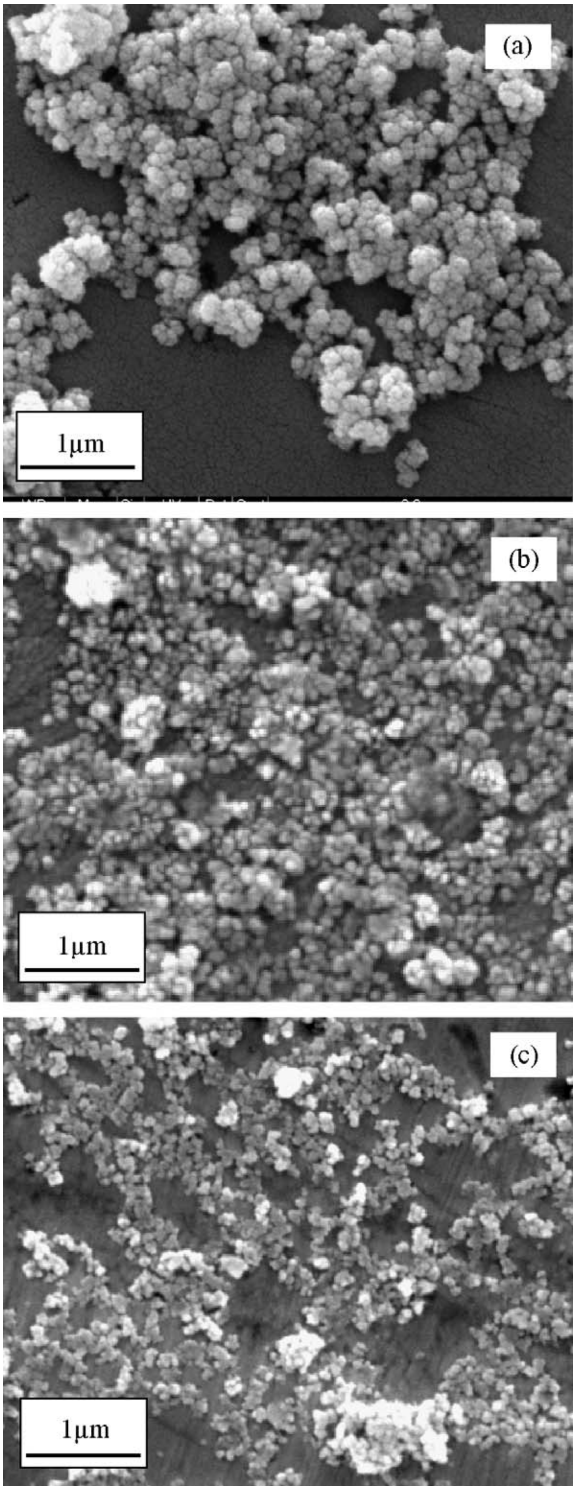

Fig. 3. SEM images of TAG samples sintered at 1100 °C (a) vacuum (~10^{-6} mbar) furnace, (b) air/furnace and (c) air/laser irradiation.

3.2. Optical properties

Room temperature excitation spectra in the region 300–500 nm have been recorded using Xe lamp as excitation source. A typical spectrum of air-sintered (furnace) is shown in Fig. 6 while the observed absorption lines along with the transition assignments are summarized in Table 1. These observed

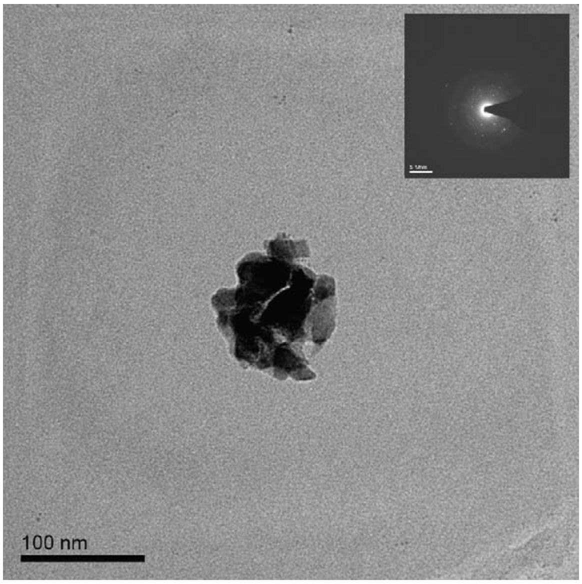

Fig. 4. Typical FETEM micrograph of TAG sample sintered at 1100 °C. The inset shows the diffraction pattern of the particle corresponding to the sample.

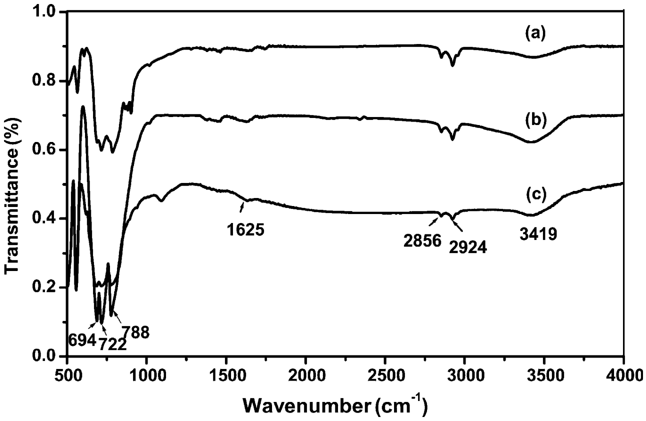

Fig. 5. FTIR spectra of TAG sintered at 1100 °C (a) vacuum (~10^{-6} mbar) furnace, (b) air/furnace and (c) air/laser irradiation.

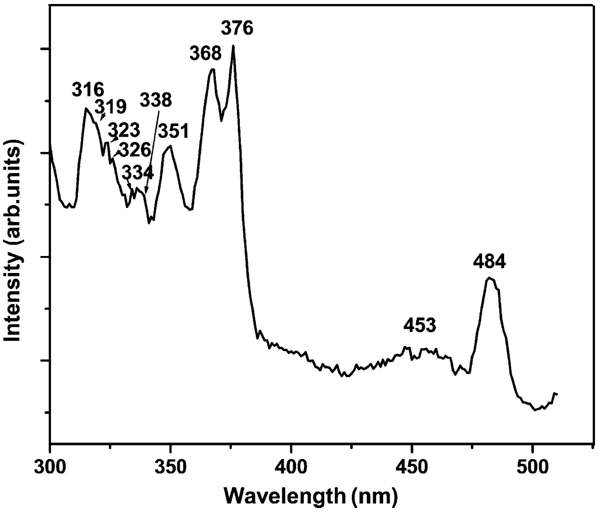

Fig. 6. Typical excitation spectrum of TAG sintered at 1100 °C in air/furnace.

Table 1
Excitation spectrum and the transition assignments of TAG sample sintered at 1100 °C in air/furnace.

λ (nm)	ν (cm^{-1})	Transition
316	31,645	$^7F_6 \rightarrow {}^5D_2$
319	31,347	
323	30,959	
326	30,674	
334	29,940	
338	29,585	
351	28,490	
368	27,173	$^7F_6 \rightarrow {}^5L_{10}$
376	26,595	
453	22,075	$^7F_6 \rightarrow {}^5D_4$

absorption lines are due to Tb^{3+} in TAG. The free-ion ground state [9] of Tb^{3+} is $^7F_6$ while the first excited state $^7F_5$ is ~2000 cm^{-1} higher to the ground state. These free-ion energy levels are (2J + 1) fold degenerate and this degeneracy is fully/ partially removed depending on the site symmetry of Tb in TAG. Since the energy (~2000 cm^{-1}) of the first excited state ($^7F_5$) is more than kT (~210 cm^{-1}, k is Boltzmann constant and T is room temperature) the absorption at room temperature takes place from the ground state $^7F_6$ only. Also, the absorption at 484 nm is interesting for the white-light emitting application.

All the observed spectral features of the excitation spectra except the absorption intensity are almost similar in the case of the TAG samples sintered in air/vacuum by furnace/CO_2 laser. The integrated intensity of the excitation spectrum of the samples sintered in vacuum is ~5.3 × 10^7 arbitrary units (a.u.) compared to ~2.0 × 10^6 a.u. for air-sintered (furnace) samples and 2.5 × 10^6 a.u. for the samples sintered in air by laser. This could be due to general increase in the transparency of the samples which has been reported in many studies [10].

The room temperature photoluminescence spectra have been recorded in 300–600 nm region using 350 and 484 nm radiation from a Xe lamp. This photoluminescence emission is due to Tb^{3+}. Typical spectra excited by 350 nm are shown in Fig. 7 while the emission lines along with transition assignments are summarized in Table 2. All the observed spectral features of the emission spectra except the emission intensity are almost similar in the case of the TAG samples sintered in air/vacuum by furnace/ CO_2 laser. The observations are summarized in Table 3. As seen in this table, the emission intensity of the vacuum sintered samples is higher compared to laser/furnace air-sintered samples. This could be, as is the case in case of absorption, due to general increase in the transparency of vacuum sintered sample.

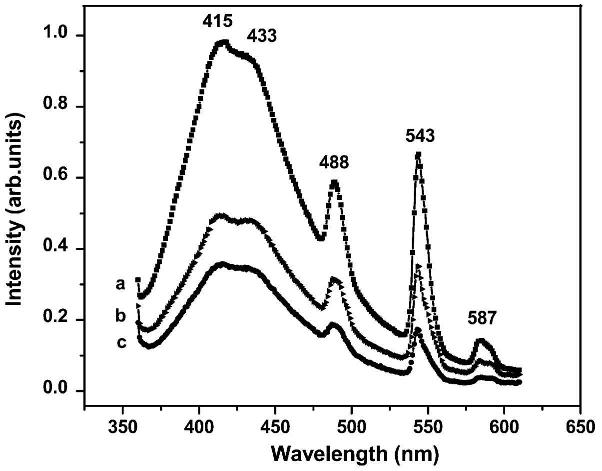

Fig. 7. Typical photoluminescence spectra (excited by 350 nm) of TAG sintered at 1100 °C (a) vacuum (~10^{-6} mbar) furnace, (b) air/laser irradiation and (c) air/furnace.

Table 2
Room temperature photoluminescence spectra (excited by 350 nm) in 300–600 nm region and transition assignments of TAG.

λ (nm)	ν (cm^{-1})	Transition
415	24,096	$^5D_3 \rightarrow {}^7F_3$
433	23,094	
488	20,491	
543	18,416	
587	17,035	

Table 3
Integrated intensities of various emission lines of TAG sintered at 1100 °C in air/vacuum (~10^{-6} mbar).

Group	Integrated intensity in arbitrary units		
	Sintered in air (in furnace)	Laser irradiated (in air)	Sintered in vacuum (in furnace)
414 nm	5.0 × 10^5	5.9 × 10^5	1.2 × 10^6
488 nm	2.3 × 10^5	3.9 × 10^5	7.1 × 10^5
543 nm	2.5 × 10^5	4.2 × 10^5	8.0 × 10^5
584 nm	4.3 × 10^4	1.0 × 10^5	1.7 × 10^5

4. Conclusions

Structural features of the TAG samples air/vacuum sintered by furnace/laser are almost similar while the absorption/ emission intensity is higher for vacuum sintered samples. However, the sintering by laser is faster (~2 h) compared to furnace; 8 h for air sintering and 4 h for vacuum sintering.

Acknowledgements

One of the authors, Humyra Shabir, gratefully acknowledges the financial support from the Department of Science & Technology, Govt. of India, New Delhi.

References

[1] C.B. Rubinstein, L.G. Van Uitert, W.H. Grodkiewicz, Magneto-optical properties of rare earth (III) aluminum garnets, J. Appl. Phys. 35 (1964) 3069–3070.

[2] F.J. Sansalone, Compact optical isolator, Appl. Optics 10 (10) (1971) 2329–2331.

[3] S. Ganschow, D. Klimm, P. Reiche, R. Uecker, On the crystallization of terbium aluminum garnet, Cryst. Res. Technol. 34 (1999) 615–619.

[4] S. Saxena, A. Asokkumar, B. Lal, Citrate–nitrate route for the synthesis and characterization of TAG using sol–gel techniques, J. Sol–Gel Technol. 45 (2007) 245–248.

[5] H. Shabir, B. Lal, M. Rafat, Synthesis and photoluminescence properties of nanocrystalline terbium aluminum garnet phosphor, Int. J. Nano Biomater. 2 (2009) 416.

[6] Y. Tang, A.C. Sutorik, L. Nguyen, T. Hinklin, W.H. Rhodes, D. Scerbak, US Patent 2007/0238604 A 1, Oct. 11 (2007).

[7] M. Veith, S. Mathur, A. Kareira, M. Jilavi, M. Zimmer, V. Huch, Low temperature synthesis of nanocrystalline $Y_3Al_5O_{12}$(YAG) and Ce-doped $Y_3Al_5O_{12}$ via different sol–gel methods, J. Mater. Chem. 9 (1999) 3069.

[8] Y.H. Zhou, J. Lin, S.B. Wang, H.J. Zhang, Preparation of $Y_3Al_5O_{12}$:Eu phosphors by citric gel method and their luminescent properties, Opt. Mater. 20 (2002) 13.

[9] D. Boal, P. Grunberg, Koningstein, Electronic Raman spectra: crystal field in terbium aluminum garnet and europium gallium garnet, Phys. Rev. B 7 (11) (1973) 4757–4763.

[10] B.D. Joshi, A.G. Page, Spectrum of Tb^{3+} ion in terbium aluminum garnet, J. Lumin. 6 (1973) 441–448.